Published in final edited form as:
Cell. 2012 December 7; 151(6): 1319–1331. doi:10.1016/j.cell.2012.10.050.

A PGC-1α isoform induced by resistance training regulates skeletal muscle hypertrophy

Jorge L. Ruas[1,5,7,*], **James P. White**[1,5], **Rajesh R. Rao**[1], **Sandra Kleiner**[1,6], **Kevin T. Brannan**[1,6], **Brooke C. Harrison**[2,6], **Nicholas P. Greene**[3], **Jun Wu**[1], **Jennifer L. Estall**[1], **Brian A. Irving**[4], **Ian R. Lanza**[4], **Kyle A. Rasbach**[1], **Mitsuharu Okutsu**[3], **K. Sreekumaran Nair**[4], **Zhen Yan**[3], **Leslie A. Leinwand**[2], and **Bruce M. Spiegelman**[1,*]

[1]Department of Cell Biology, Dana-Farber Cancer Institute, Harvard Medical School, Boston, Massachusetts 02115, USA

[2]Department of Molecular, Cellular, and Developmental Biology, University of Colorado at Boulder, Boulder, CO 80309, USA

[3]Department of Medicine-Cardiovascular Medicine, University of Virginia, Charlottesville, VA 22908, USA

[4]Division of Endocrinology, Endocrine research Unit, The Mayo Clinic, 200 1st Street SW Joseph 5-194, Rochester, MN 55905, USA

SUMMARY

PGC-1α is a transcriptional coactivator induced by exercise that gives muscle many of the best known adaptations to endurance-type exercise, but has no effects on muscle strength or hypertrophy. We have identified a novel form of PGC-1α (PGC-1α4) that results from alternative promoter usage and splicing of the primary transcript. PGC-1α4 is highly expressed in exercised muscle but does not regulate most known PGC-1α targets such as the mitochondrial OXPHOS genes. Rather, it specifically induces IGF1 and represses myostatin, and expression of PGC-1α4 *in vitro* and *in vivo* induces robust skeletal muscle hypertrophy. Importantly, mice with skeletal muscle-specific transgenic expression of PGC-1α4 show increased muscle mass and strength, and dramatic resistance to the muscle wasting of cancer cachexia. Expression of PGC-1α4 is preferentially induced in mouse and human muscle during resistance exercise. These studies identify a novel PGC-1α protein that regulates and coordinates factors involved in skeletal muscle hypertrophy.

INTRODUCTION

PGC-1α is a transcriptional coactivator that controls the expression of genes involved in oxidative metabolism. PGC-1α was originally identified as a coactivator of PPARγ in brown adipose tissue but it is enriched in many tissues that are active in oxidative metabolism, such as heart, skeletal muscle and the fasted liver. Muscle PGC-1α is induced

*Correspondence to: jorge.ruas@ki.se or bruce_spiegelman@dfci.harvard.edu.
[5]These authors contributed equally to this work.
[6]These authors contributed equally to this work.
[7]Present address: Department of Physiology and Pharmacology, Karolinska Institutet, S-171 77, Stockholm, Sweden.

by exercise in both mice and humans (Short et al., 2003). When expressed in skeletal muscle *in vivo*, PGC-1α causes many of the changes associated with endurance training, including mitochondrial biogenesis, fiber-type switching, stimulation of fatty acid oxidation, angiogenesis and resistance to muscle atrophy (Arany, 2008). This reprogramming of muscle results in increased muscle endurance. Genetic loss of PGC-1α in murine muscle causes glucose intolerance, especially on a high fat diet (Choi et al., 2008; Handschin et al., 2007). Elevated PGC-1α in muscle does not protect against insulin resistance stimulated by a high fat diet in young mice (Choi et al., 2008) but dramatically protects against the sarcopenia, obesity and diabetes that accompanies aging (Wenz et al., 2009). Although PGC-1α is induced in exercise and has remarkable effects on muscle endurance, it has no clear-cut effects on either muscle size or strength. Here we identify a new transcript from the PGC-1α gene that is expressed abundantly in skeletal muscle, particularly in the setting of resistance training in mice and humans. This protein, termed PGC-1α4, does not regulate the same set of genes induced by PGC-1α but rather regulates the IGF1 and myostatin pathways, both of which are known regulators of muscle size and strength (Florini, 1987; McPherron et al., 1997). This results in muscle hypertrophy and increased strength. Remarkably, mice with skeletal muscle-specific transgenic expression of PGC-1α4 show a dramatic resistance to the muscle wasting of cancer cachexia. Taken together, these data suggest that PGC-1α4 integrates resistance training with a gene program of muscle hypertrophy, which results in several important health benefits.

RESULTS

Identification, characterization and expression of alternative isoforms of PGC-1α

We and others have shown that transcription of the PGC-1α gene can be driven by two distinct promoter regions (Chinsomboon et al., 2009; Yoshioka et al., 2009). One is located immediately 5’ of the known exon1 (proximal promoter) and another (alternative promoter) is located approximately 13 Kb upstream (Figure 1A). Using a targeted PCR strategy (Figure S1A), we cloned and characterized the transcripts that result from the use of either promoter in mouse skeletal muscle. We cloned four full-length mRNAs; one of these corresponds to the previously described PGC-1α (hereafter referred to as PGC-1α1) and originates exclusively from the proximal promoter. The other three transcripts (hereafter referred to as PGC-1α2, α3, and α4) result from alternative promoter usage, and alternative splicing of the PGC-1α gene (Figures 1A and S1C). The new isoforms encode significantly different proteins (Figure 1B). PGC-1α2 and α3 have distinct first exons, but the same remaining exon/intron structure (Figure S1C); this results in two new proteins with overall similar domain structure but discrete N-termini (Figure 1C). PGC-1α2 and α3 are 379 and 370 amino acids long, and have a predicted molecular weight of 41.9 and 41.0 kDa, respectively. PGC-1α4 shares the same alternative exon1 with PGC-1α2 (and therefore same N-terminus, Figure 1C) but its mRNA structure is different in that it contains a 31 nucleotide insertion between exons 6 and 7 which generates a premature stop codon (Figures 1A-B and S1C). PGC1α4 is predicted to encode 266 amino acids, a protein of 29.1 kDa. The different alternative first exons generate different N-termini that seem to significantly affect protein accumulation (Figures 1C-D and S1B). With the use of specific qPCR probes, we determined total PGC-1α mRNA content (targeting exon 2, which is present in all forms), or the expression of each individual isoform in an array of mouse tissues (Figure 2A). In fed liver, PGC-1α1 levels approach total PGC-1α content, and no significant alternative isoform expression is observed (Figure 2A). However, in skeletal muscle, heart, and brown adipose tissue (BAT) all isoforms are expressed at comparable levels and represent a significant part of total PGC-1α mRNA. Figure S2A and B show PGC-1α isoform protein levels in superficial white quadriceps (glycolytic, low PGC-1α1 levels), tibialis anterior (oxidative, high PGC-1α1 levels) muscle, as well as liver, kidney and BAT.

Primary myotubes treated with the known PGC-1α inducer forskolin show high levels of all isoforms (Figure S2C). Similarly, cold exposure induces expression of all PGC-1α variants in BAT (Figure S2DE). These results show that total PGC-1α mRNA content includes significant levels of each isoform, which can be increased *in vitro* and *in vivo* by known inducers of the PGC-1α gene.

PGC-1α4 regulates a discrete gene program in primary myotubes

Differentiated primary myotubes were transduced with adenovirus expressing different PGC1α isoforms. Figure 2B shows a heat map generated by comparing the gene expression profile of cells receiving each PGC-1α isoform, compared to GFP alone. Interestingly, PGC-1α1 and PGC-1α4 drive many changes in gene expression that are distinct from each other; only 98 genes were co-regulated by both PGC-1α1 and PGC-1α4 (Figure 2C). PGC-1α2 and 3 seem to affect the expression of only a very small set of genes (110 and 69 gene IDs respectively). The functions of PGC-1α2 and α3 remain under investigation. Importantly, expression of PGC-1α4 in myotubes did not affect the regulation of many classic PGC-1α1 targets including CytC (cytochrome C), CoxVb (cytochrome c oxidase subunit Vb), Glut4 (glucose transporter type 4), CPT1 (carnitine palmitoyltransferase-I), MCAD (medium chain acyl CoA dehydrogenase) and PDGFb (platelet derived growth factor B) (Figure 2D). Several other known PGC-1α target genes were induced by PGC-1α4 expression, though to a much lesser extent than upon expression of PGC-1α1 (Figure 2D), including ERRα, PDK4 (pyruvate dehydrogenase kinase, isoenzyme 4) and VEGFa (vascular endothelial growth factor A). These results strongly suggest distinct functions for PGC-1α1 and PGC1α4.

Expression of PGC-1α4 specifically induces IGF1 and represses myostatin gene expression

Pathway analysis of the microarray data identified cell morphology, growth and proliferation, and IGF1 signaling as the top pathways predicted to be under PGC-1α4 regulation (data not shown). From qRT-PCR, we confirmed that PGC-1α4 (but not α1), specifically induces expression of IGF1 (3.7-fold) while minimally affecting IGF2 (1.5-fold) levels (Figure 2E). The expression levels of some members of the IGF binding protein (IGFBP) family were also selectively affected by PGC-1α4 expression. IGF1 is among the best-known activators of skeletal muscle hypertrophy (Adams, 2002). PGC-1α4 expression also reduced mRNA levels of myostatin, a powerful, negative regulator of muscle size in rodents and humans (Figure 2F; (Lee, 2004; McPherron et al., 1997), as well as the transcript levels of its receptors ACVRIIa and ACVRIIb (40% and 30%, respectively). The levels of ACVRIb remained unaffected by expression of either PGC-1α1 or PGC1α4, whereas both isoforms repress follistatin expression (Figure 2F). Taken together, these results indicate that PGC-1α4 controls the expression of genes in two important pathways for regulating skeletal muscle size.

PGC-1α4 expression leads to powerful myotube hypertrophy

Myotubes expressing PGC-1α4 appear significantly larger than those expressing GFP control or PGC-1α1 (Figure 3A), with a 2-fold elevation in the ratio of total protein to genomic DNA (Figure 3B). We observed no significant differences in fusion of myoblasts expressing GFP or the different PGC-1α isoforms, as assessed by the number of nuclei per myotube (Figure S3A). Importantly, the PGC-1α4-dependent increase in myotube size and protein accumulation could be inhibited by an IGF1 receptor (IGF1R) inhibitor (BMS-754807,(Dinchuk et al., 2010)) (Figures 3C and S3B). Under the same conditions, no significant changes in total protein accumulation were observed in cells expressing GFP or PGC-1α1. Although we observed an increase in expression of the myogenic transcription factors Myf5 and 6, the levels of MyoD and myogenin were only minimally affected (Figure

3D). Small effects were also observed in the expression of the atrophy-related genes MuRF-1 and atrogin-1/MAFbx (Figure 3D) (Bodine et al., 2001; Gomes et al., 2001). Both PGC-1α isoforms show a predominantly nuclear localization in skeletal myotubes (Figure S3C). Taken together, these results clearly suggest a role for PGC-1α4 in the regulation of myotube size and protein content, mediated (at least in part) by IGF1.

PGC-1α4 loss-of-function blunts skeletal muscle cell hypertrophy in culture

To evaluate the requirement for PGC-1α4 in a cellular model of skeletal muscle hypertrophy, we developed an isoform-specific shRNA. As shown in Figure S3D, PGC 1α4 shRNA efficiently reduces PGC-1α4 mRNA levels in transduced myotubes, while not affecting PGC-1α1. Myotube hypertrophy was induced by treatment with the β-adrenergic agonist clenbuterol (McMillan et al., 1992); this resulted in robust hypertrophy (Figure 3E) accompanied by a 5-fold increase in endogenous PGC-1α4 levels, and in a 1.9-fold increase in protein/DNA ratio (Figure S3D-E). No changes were observed in PGC-1α1 levels with clenbuterol treatment. However, shRNA-mediated reduction in PGC-1α4 levels blunted clenbuterol-induced myotube hypertrophy (Figure 3E) and protein accumulation, compared to a scrambled control (Figure S3E). These results show that PGC-1α4 is required for myotube hypertrophy in this cellular model.

Loss of estrogen-related receptors α or γ does not affect PGC-1α4-mediated myotube hypertrophy

The estrogen-related receptors are master drivers of OXPHOS gene expression under PGC-1α1 coactivation (Giguere, 2008). We investigated if myotubes genetically deficient in ERRα or ERRγ could still support PGC-1α4 function. Differentiated myotubes were transduced with adenovirus expressing GFP control or PGC-1α4 and even in the absence of ERRα PGC-1α4 was still able to induce robust myotube hypertrophy (Figure S4F); both IGF1 and myostatin genes were regulated as previously observed in wild-type cells (Figure S3G). Similar results were obtained with ERRγ-defficient myotubes (data not shown). In agreement with these results, and in contrast to PGC-1α1, PGC-1α4 did not coactivate ERRα function in luciferase assays using two different reporters for ERR-mediated transactivation. (Figure S3H). These results indicate that PGC-1α4 does not coactivate ERR function, which likely contributes to the lack of effect on OXPHOS gene expression.

PGC-1α4 expression induces changes in histone modifications near the IGF1 and myostatin genes

The PGC-1s have been shown to associate with other coregulatory complexes to promote chromatin remodeling and enhance transcription of target genes (Lin et al., 2005). One such complex is anchored by the histone acetyltransferase CBP/p300, which mediates histone tail acetylation as a mark for positive gene regulation (Ogryzko et al., 1996). Since IGF1 gene transcription is enhanced by PGC-1α4 we performed chromatin immunoprecipitation (ChIP) experiments using an anti-acetyl-H3K9 antibody to identify potential IGF1 gene enhancer regions. We thus identified three regions of DNA where association with acetyl-H3K9 was significantly enriched upon expression of PGC-1α4 (Figure 3F). Those included the gene promoter (2.7-fold) and 3'UTR (3.3-fold), and a region located 4 kb upstream of the transcription initiation site (5.9-fold). To identify regions of the myostatin gene that could mediate the repressive effect of PGC1α4, we performed ChIP experiments targeting DNA regions associated with di/trimethyl-H3K9, a mark for negative gene regulation (Heard et al., 2001). Of the identified regions, a sequence located 5 kb upstream of the myostatin gene showed the highest PGC-1α4-induced association with di/trimethyl-H3K9 (74.3-fold) (Figure 3G), suggesting the potential location of a regulatory region. Upon expression of PGC-1α4, the 3'UTR of the myostatin gene showed a 3.2 fold higher association with di/tri-methyl-H3K9 whereas the gene promoter showed a decrease of 80%. These results identify

putative regulatory regions near the IGF1 and myostatin genes, which could be the target of PGC-1α4-mediated regulation.

Delivery of PGC-1α4 to skeletal muscle causes marked hypertrophy *in vivo*

To evaluate the effect of PGC-α4 expression *in vivo*, we performed intramuscular injections of the adenoviral vectors. Mice with Severe Combined Immunodeficiency (SCID) were used to maximize adenovirus uptake by muscle and reduce any immune response to the adenoviruses (Chakkalakal et al., 2010). Each mouse received an injection of GFP control adenovirus into the gastrocnemius of one limb (Figure S4A), and an equivalent injection of a PGC-1α4-expressing adenovirus into the contralateral limb. Seven days after injection, fibers expressing PGC-1α4 showed a 59.5% increase in average cross sectional area (CSA), compared to controls (Figure 4A and S4B). In particular, PGC1α4 drove the appearance of very large fibers (in the >1200 μm^2 interval) that were rarely seen with the control (Figure 4B). PGC-1α4 expression *in viv*o resulted in a 2.3-fold increase in IGF1 gene expression and in a 50% reduction in myostatin gene expression (Figure S4C). Furthermore, PGC-1α4 expression in muscle resulted in increased S6 ribosomal protein phosphorylation levels (Figure S4D), indicative of S6K activation (Pende et al., 2004).

We also performed electroporation of plasmids encoding PGC-1α4 (or a control) into the tibialis anterior of C57Bl/6 mice. As before, each mouse received the control plasmid in one limb, and the PGC-1α4-expression plasmid in the contralateral limb. Recently, another PGC-1α splicing variant has cloned from a mouse brown adipose tissue cDNA library and named NT-PGC-1α (Zhang et al., 2009). Although we have been unable to detect expression of endogenous NT-PGC-1α transcript in skeletal muscle, we tested if electroporation of a plasmid encoding this PGC-1α variant would induce changes in the CSA of targeted fibers, as observed for PGC-1α4. Although PGC-1α4 and NT-PGC-1α mRNAs were expressed at similar levels (Figure 4C), we could not detect NT-PGC-1α protein accumulation by immunoblotting (Figure 4D). We observed an average increase of 28% in CSA of PGC-1α4 expressing fibers when compared to controls (Figure S4E). Results are also shown as CSA frequency distribution in Figure 4E and show a 34.7% reduction in the smallest CSA interval (<1000 μm^2), and increases of 45.5% and 99.4% in the -2000 and -2500 μm^2 intervals (respectively). As before, we observed fibers of CSA in the -3000 and >3000 μm^2 intervals, which were not significantly observed in controls (Figure 4E). This increase in average CSA was accompanied by a 10% increase in muscle weight, compared to control limb (Figure S4F). PGC-1α4 expression resulted in higher phospho-S6K levels (Figure S4G). Expression of NT-PGC-1α resulted in a decrease of 46.7% and 66.9% in the number of larger fibers with CSA in the -2000 and -2500 μm^2 intervals (respectively), and an increase of 33.8% in smaller fibers with CSA in the -1500 μm^2 interval (Figure 4F). These results indicate that *in vivo* delivery of PGC-1α4 results in a marked increase in the CSA of targeted fibers.

Regulation of PGC-1α4 expression during hindlimb suspension/reloading

We next investigated whether PGC-1α4 levels are regulated by a hindlimb suspension/ reloading protocol, a model of skeletal muscle hypertrophy in rodents (Hanson et al., 2010). As shown in Figure 5A, hindlimb suspension resulted in a small but significant decrease in total PGC-1α content in the soleus muscle (0.85-fold when compared to control), and reloading in a 1.6-fold increase. Changes in muscle wet weights are shown in Figure S5A. No significant changes in PGC-1α1 mRNA levels were observed upon suspension, but a marked reduction was seen after reloading (50% vs. control), when hypertrophic signaling cascades are initiated. Accordingly, during the suspension and reloading phases, we observed a reduction in the expression of transcripts driven by the proximal promoter of the PGC-1α gene, as assessed by qRT-PCR using primers directed at that 5'UTR region (Figure

S5B). Interestingly, PGC-1α4 expression levels drop to 22% of starting levels after suspension, and increase by 18.7-fold with reloading (Figure 5A). The increase in PGC-1α4 mRNA expression during the reloading phase was accompanied by significant protein accumulation (Figure S5C). This expression pattern matches the suspension/atrophy and reloading/hypertrophy phases and coincided with an increase in IGF1 and a decrease in myostatin gene expression (1.8-fold and 40%, respectively, Figure 5B). Similar results were obtained with the gastrocnemius/plantaris muscles (Figure S5A and D).

Different exercise protocols result in differential PGC-1α isoform expression in human muscle

We determined the expression of PGC-1α4 in human skeletal muscle with training. Percutaneous muscle biopsies of the vastus lateralis muscle were obtained at baseline and 48 h after the last training session. Figure 5C shows the change in total PGC-1α expression at the end of the indicated exercise protocol. All exercise programs elevated total PGC-1α levels in muscle, although to different degrees. Notably, the combined endurance/resistance protocol induced the most significant increase in PGC-1α expression. We observed no changes in PGC-1α4 expression in the endurance protocol group (Figure 5D). However, both the resistance and the combined exercise programs led to a 1.5-and 3-fold increase in the expression of PGC-1α4 (respectively). We observed a reduction in myostatin gene expression only in the resistance and combined groups (Figure 5E), but no statistically significant changes in IGF1 expression (Figure 5F). Interestingly, a very significant correlation across all groups (R=0.64) was observed between the changes in PGC-1α4 expression and performance in the leg press exercise (Figure 5G).

Transgenic muscle-specific expression of PGC-1α4 drives increased muscle mass, strength and reduced adiposity

To evaluate the effects of chronically elevated PGC-1α4 levels in muscle, we generated the transgenic mouse model Myo-PGC-1α4. This mouse (Figure 5H), expresses PGC-1α4 under the control of a MEF2C enhancer/myogenin promoter (Li et al., 2005); the muscles had 30-fold above endogenous levels (Figure 5I) and resulted in significant PGC-1α4 protein accumulation (Figure 5H). Importantly, these levels of expression bring PGC-1α4 levels up to those observed during the reloading phase of the suspension/reloading experiments (i.e. 19-fold, Figure 5A). Analysis of the Myo-PGC-1α4 mouse shows redder muscle when compared to the wild-type littermate controls (Figure 5H). The pattern of gene expression observed in the muscle of Myo-PGC-1α4 mice (Figure S5E) was similar to the one observed upon expression of PGC-1α4 in myotubes (Figures 2DF) with the exception of IGF1. In these animals, and consistent with our previous results, we observed a 64.4% reduction in myostatin expression. However, there was no increase in IGF1 expression (Figure S5E). PGC-1α4 transgenic mice showed an increase in muscle wet weight as observed in Figure 6A. The increase in muscle mass was accompanied by an average increase of 12% in fiber CSA (Figure 6B), with a significant increase in larger fibers (Figure S6A-B). Analysis of myosin heavy chain expression in transgenic muscle, revealed a higher representation of type IIa and IIx fibers at the expense of IIb (Figure 6C and S6C). Interestingly, these animals also show reduced adiposity. Skeletal muscle-specific PGC-1α4 transgenics show a reduction of 20.7% and 40% in the mass of the epididymal and retroperitoneal fat depots (Figure 6D). Among the tissues analyzed, this observation proved to be selective to fat (Figure S6D). When compared to the wild-type controls, the PGC1α4 transgenics show a 20% increase in maximum force generated (Figure 6E). Interestingly, transgenic muscle also proved to be more fatigue-resistant than wild-type (Figure 6F). These results show that elevation of PGC-1α4 levels in skeletal muscle results in a hypertrophy phenotype accompanied by a significant increase in strength.

Myo-PGC-1α4 mice show less muscle loss upon hindlimb suspension, and improved exercise performance

To evaluate the physiological alterations in the Myo-PGC-1α4 mouse, we performed hindlimb suspension/reloading experiments. Myo-PGC-1α4 mice loss significantly less muscle mass during the suspension phase (Figure 6G), and trended towards accumulating more muscle mass during the reloading process. Myo-PGC-1α4 mice were evaluated for their performance on an exercise tolerance test and compared to littermate controls and to the previously reported mice with muscle-specific PGC-1α1 expression (MCK-PGC-1α). As expected (Lin et al., 2002), MCK-PGC-1α mice remained on the treadmill 60% longer than controls (Figure 6H). The Myo-PGC-1α4 mice showed improved performance, with a 28% increase in time to exhaustion compared to controls (Figure 6H). No differences in glucose tolerance were observed between these mouse models and controls (Figure S6E). Metabolic profiling of the Myo-PGC-1α4 mice using Comprehensive Laboratory Animal Monitoring System (CLAMS) revealed that although these animals have higher maximum oxygen consumption (VO_2) and carbon dioxide elimination (VCO_2), their respiratory exchange ratio (RER) is unchanged (Figure S6F). No changes in food consumption (Figure S6F) or movement (data not shown) were observed. These results show that the increase in muscle mass and strength observed in the Myo-PGC-1α4 mice does not result in an overt metabolic phenotype, but contributes to better exercise performance and protects against hindlimb unloading-induced atrophy.

Myo-PGC-1α4 mice show resistance to cancer-induced cachexia with improved glucose tolerance and preserved muscle mass

Cancer cachexia is a very important complication of many malignancies, resulting in severe muscle wasting and negatively affecting patient outcome (Fearon et al., 2012). Wild-type and Myo-PGC-1α4 mice were inoculated with the Lewis Lung Carcinoma (LLC) cells and the cachectic phenotype was evaluated 24–28 days after inoculation. Importantly, this model of cachexia is characterized by loss of muscle mass and strength, and development of glucose intolerance (Busquets et al., 2012; Das et al., 2011). Upon necropsy analysis of tumor-bearing animals, muscles of Myo-PGC-1α4 mice looked less pale and healthier when compared to cachectic muscle from wild-type mice (Figure 7A). Strikingly, tumor-bearing Myo-PGC-1α4 mice lost only 10% of gastrocnemius muscle mass (Figure 7B), compared to wild-type tumor-bearing animals (29%). This was accompanied by improvements in both muscle force production and myofiber cross sectional area (Figures 7C and S7A). Cancer-induced cachexia has been shown to occur concomitantly with dysregulation of myostatin and IGF1 expression in muscle (Busquets et al., 2012; Fearon et al., 2012; White et al., 2011). Analysis of muscle gene expression in the different groups revealed that cachectic wild-type animals indeed have a 2.2-fold increase in myostatin gene expression but only a 1.2-fold increase was seen in tumor-bearing Myo-PGC-1α4 animals (Figure 7D). Conversely, IGF1 gene expression was 59% lower in cachectic wild-type muscle whereas the corresponding Myo-PGC-1α4 mice showed only a 27% reduction (Figure 7D). SMAD phosphorylation, a marker of myostatin signal transduction, was clearly suppressed in the Myo-PGC-1α4 mice (Figure S7B). The expression of other muscle wasting markers such as MuRF1 and atrogin1/MAFbx1 (Figure S7C) were also strongly reduced in cachectic Myo-PGC-1α4 mice (2.3- and 1.9-fold, respectively) when compared to wild-type tumor-bearing controls (5.6- and 7-1-fold, respectively). Tumors in both genotypes of mice grew at the same rates (Figure S7D). Wild-type and Myo-PGC-1α4 mice were studied throughout the development of the cachexia phenotype for physical activity, glucose tolerance and food consumption. No changes in food intake were observed between wild-type and Myo-PGC-1α4 mice with or without LLC cell inoculation (Figure S7E). While physical activity was similar between wild-type and Myo-PGC-1α4 mice before the inoculation of the cancer cells (Figure 7E), it declined more strongly with tumor load in wild-type than in Myo-

PGC-1α4 mice (Figure 7E). Tumor-bearing Myo-PGC-1α4 mice displayed improved glucose tolerance compared to cachectic wild-type mice, as shown by their ability to clear a bolus of glucose (Figure 7F-G). Thus, transgenic expression of PGC-1α4 in muscle dramatically ameliorates cancer-induced cachexia through reduced loss of muscle mass and strength, and improved glucose homeostasis during cancer progression.

DISCUSSION

Exercise is usually considered in two broad categories: endurance training, which involves low resistance work of longer duration, and resistance training, which requires more powerful movements of shorter duration. Health studies suggest that most humans should participate in both types of exercise, especially in aging populations (Nair, 2005). Molecular mechanisms underlying the different exercise modalities are not well understood but the importance of maintaining muscle mass and strength as humans age has motivated considerable research into the pathways of muscle growth; these have highlighted the importance of the IGF1 and myostatin systems (Schiaffino and Mammucari, 2011) (Lee, 2004; McPherron et al., 1997). PGC-1α, now termed PGC-1α1, is induced by exercise and regulates many of the effects of endurance training: mitochondrial biogenesis, fiber-type switching, angiogenesis and resistance to muscle atrophy. However, gain of function studies with PGC-1α have not shown any increase in either muscle mass or strength (Lin et al., 2002; Sandri et al., 2006; Wende et al., 2007). Similarly, other PGC-1α variants have been shown to specifically affect energy metabolism in brown adipose tissue and skeletal muscle, but no effects on cell size have been reported (Tadaishi et al., 2011; Yoshioka et al., 2009; Zhang et al., 2009).

Here we show that the PGC-1α gene encodes a new protein (PGC-1α4) that is expressed robustly in muscle and particularly induced by resistance training. The PGC-1α gene has been shown to be subject to alternative splicing, but the PGC-1α4 isoform is undescribed. It is somewhat similar to the NT-PGC-1α isoform (Zhang et al., 2009), but PGC-1α4 comes from a different gene promoter and has a completely distinct N-terminus derived from the upstream exon 1. Our data strongly suggest that the distinct N-terminal sequence of the PGC-1α4 is important in allowing this protein to accumulate in skeletal muscle and perhaps in other tissues.

PGC-1α4 specifically activates the expression of IGF1 and suppresses myostatin in skeletal muscle. That the net result of PGC-1α4 expression in cultured myotubes represents *bona fide* hypertrophy, as opposed to hyperplasia, can be deduced from the fact that protein content per unit DNA doubles. In a classical cellular system of muscle cell hypertrophy, stimulation with clenbuterol, PGC1α4 is required for this increase in myotube size. PGC-1α4 also induces muscle fiber hypertrophy *in vivo* in three independent expression systems used here: transduction with adenoviral vectors, delivery of naked DNA, and transgenic expression with a muscle-selective promoter. All of these systems give very comparable results, with muscle fiber hypertrophy, modulation of myostatin expression and in some cases, increases in IGF1 expression. Importantly, we see no changes in mitochondrial gene expression, which is a virtual hallmark of PGC-1α1 expression in skeletal muscle. This could be partly explained by the fact that PGC-1α4 does not robustly coactivate ERRs.

Transgenic mice with an increase in PGC-1α4 expression within or close to the physiological range results in a 60% decrease in myostatin mRNA expression. This is comparable to the 50% decrease observed in mice heterozygous for a null mutation in the myostatin gene. Muscle mass changes in myostatin heterozygous mice range from 7 to 35%, depending on the muscle type and study (Gentry et al., 2011; Lee, 2007; Mendias et al.,

2006). The changes observed in the Myo-PGC-1α4 mouse are comparable to those reported in two of those studies (Gentry et al., 2011; Mendias et al., 2006). While effects on other molecular systems are entirely plausible, the effect of PGC-1α4 on myostatin gene expression is likely to be a major contributor to the phenotype seen in the Myo-PGC-1α4 animals.

Importantly, PGC-1α4 transgenic mice to have an increase in muscle force production proportional to the increase in muscle mass, indicating forced PGC-1α4 expression in muscle results in functional hypertrophy. The increase in muscle mass and strength results in other significant functional consequences, including exercise tolerance, and resistance to hindlimb suspension-induced muscle atrophy. The transgenic expression of PGC-1α4 also had a strikingly protective effect in the pathogenesis of cancer-induced cachexia. While tumors grew at an equal rate in mice of both genotypes, tumor-bearing Myo-PGC-1α4 mice lose less muscle mass and strength than controls, and do not develop the glucose intolerance observed in the cachectic control animals. This protective effect is clearly reflected in the spontaneous physical activity of the tumor-bearing transgenic animals, which approaches that of non-tumor-bearing wild-type controls, even in the most severe phases of tumor development.

Since PGC-1α4 contains the complete activation domain also present in PGC-1α1, it seems highly likely that PGC-1α4 also functions as a coactivator. However, since PGC-1α1 does not stimulate IGF1 and myostatin gene expression, PGC-1α4 may be interacting with a very different set of DNA-binding proteins. Interestingly, histone deacetylase (HDAC) inhibition can induce muscle hypertrophy (Iezzi et al., 2004) through a mechanism that involves induction of follistatin expression and increased myoblast recruitment and fusion. Follistatin is a negative regulator of myostatin action and therefore acts positively on muscle mass independent of the IGF1 pathway (Iezzi et al., 2004). We have observed a reduction in follistatin mRNA levels upon PGC-1α4 expression (Figure 2F), which would suggest it does not contribute to PGC-1α4-induced muscle hypertrophy. In agreement with this result, PGC-1α4 can promote myotube hypertrophy without an increase in myoblast fusion (Figure S3A).

Finally, the potential of PGC-1α4 in therapeutics seems obvious. Loss of muscle mass and strength in aging, wasting diseases and in certain muscular dystrophies affect both quality of life and longevity. While protein therapeutics for both the IGF1 and the myostatin pathways are being developed, PGC-1α4 can, in principle, modulate both of these systems in a highly coordinated way. Since PGC-1α4 comes from a distinct promoter with some degree of distinct regulation *in vivo*, it will be important to find chemical matter that can modulate PGC-1α4 gene expression. In addition, PGC-1α4 gene expression might be used as a helpful readout for optimizing resistance training that focuses on increasing muscle strength.

EXPERIMENTAL PROCEDURES

PGC-1α isoform cloning and detection

PGC-1α isoforms were cloned from a mouse soleus cDNA library. Primer sequences used for cloning and for qRT-PCR detection of the different isoforms in mouse and human tissues can be found in Supplemental Experimental Procedures.

Cell culture, western blotting and immunocytochemistry

Primary satellite cells (myoblasts) were isolated, maintained, and differentiated as described previously (Megeney et al., 1996). To detect all PGC-1α variants by immunoblotting, anti-PGC-1α antibodies were obtained from Calbiochem (ST1202). For PGC-1α isoform

immunoprecipitation experiments antibodies were obtained from Santa Cruz Biotechnologies (sc-13067).

Adenovirus-mediated expression

Adenovirus expressing the different mouse PGC1α isoforms or GFP were generated using the pAdTrack/pAdEasy system (Stratagene). For cell culture experiments differentiated myotubes were transduced with an adenovirus at an MOI of 100 overnight. For intramuscular delivery of adenovirus, PGC1α4 or GFP viral stock (10 μl, 2×10^{10} infectious particles) was injected into the lower limbs of young SCID mice. Each mouse received the control adenovirus in one limb and the PGC-1α4 in the contralateral limb. Tissues were harvested seven days after injection.

Clenbuterol-induced myotube hypertrophy and PGC-1α4 knockdown

Differentiated primary myotubes were treated with 500 nM clenbuterol (Sigma) and PGC-1α4 shRNA (ATA AAT GTG CCA TAT CTT CCA) or scrambled shRNA for 48 hours. Cells were then divided in aliquots for genomic DNA and total protein quantification

Chromatin immunoprecipitation

ChIP was carried out according to a protocol from Upstate Biotechnology. Input DNA and immunoprecipitated DNA were analyzed by quantitative PCR. Primer sequences used to detect each DNA region are available upon request.

Electric pulse-mediated gene transfer

Electric pulse-mediated gene transfer was modified from previous studies (Mir et al., 1999). A detailed description can be found in Supplemental Experimental Procedures.

Fiber type and cross sectional area determination

Fiber type determination was done as previously described (Arany et al., 2007). CSA was determined with ImageJ software.

Hindlimb suspension and reloading

HS was preformed as described previously (Hanson et al., 2010). All protocols were approved by the University of Colorado Institutional Animal Care and Use Committee. A detailed description is included in Supplemental Experimental Procedures.

Human Exercise Training

Table S1 provides a complete description of the exercise programs and a detailed protocol can be found in Supplemental Experimental Procedures.

Generation of transgenic mice and animal experimentation

Generation of Myo-PGC-1α4 mice was done by cloning the PGC-1α4 cDNA in front of a MEF2C enhancer/Myogenin promoter DNA sequences (Li et al., 2005), followed by the human growth hormone polyA. Mice were maintained under standard conditions. All experiments and protocols were performed in accordance with the Dana-Farber Cancer Institute or Beth-Israel Deaconess Medical Center Animal Facility Institutional Animal Care and Use Committee regulations.

Muscle force measurements

Maximal muscle force was measured as previously described (Axell et al., 2006)with an isometric transducer (ADInstruments, Colorado Springs, CO, USA). Specific maximal force

was quantified by correcting for muscle mass. A fatigue test was performed following the maximal contractions.

Exercise Tolerance Test

Exercise tolerance was performed as previously described (Arany et al., 2007).

Cachexia studies

Wild-type and Myo-PGC-1α4 mice were given a subcutaneous injection in the left flank of either 10^7 LLC cells in PBS or PBS alone (control). Stages of tumor severity were defined as follows: Pre (before development of tumor) 1–5 day after inoculation, Moderate (moderate tumor size) 10–15 days after inoculation and Severe (large tumor size) ~23–28 days after inoculation. Mice with tumor development were sacrificed 28 days after injection.

Statistical Analysis

All results are expressed as means ± SD for cell experiments and ± SEM for animal experiments. Two-tailed Student's t test was used to determine p values. Statistical significance was defined as $p < 0.05$.

Supplementary Material

Refer to Web version on PubMed Central for supplementary material.

Acknowledgments

We thank Drs. Srikripa Devarakonda and Sibylle Jäger for valuable discussions. ERRα and ERRγ KO myoblasts were a kind gift from Dr. Zhidan Wu (Novartis Institutes for Biomedical Research). The MEF2C/Myogenin promoter cassette was kindly provided by Dr. Eric Olson (University of Texas Southwestern Medical Center). LLC cells were kindly donated by Dr. Jose M Garcia (Baylor College of Medicine). This project was supported by grants (DK061562) from the NIH and from Novartis to B.M.S. J.L.R. was supported in part by a grant from the Wenner-Gren Foundations, Sweden. This research was supported in part by grants to B.H. (NIH, 5K01AR55676-2), N.P.G. (NIH, T32HL07284), J.W. (AHA, #09POST2010078 and #12SDG8070003), B.A.H (RR024151, and AG09531), Z.Y (NIH, AR050429), and L.L. (NIH, GM29090). BMS is a shareholder and consultant to Ember Therapeutics and has received funding in the form of Sponsored Research from Novartis Inc.

REFERENCES

Adams GR. Invited Review: Autocrine/paracrine IGF-I and skeletal muscle adaptation. J Appl Physiol. 2002; 93:1159–1167. [PubMed: 12183514]

Arany Z. PGC-1 coactivators and skeletal muscle adaptations in health and disease. Curr Opin Genet Dev. 2008; 18:426–434. [PubMed: 18782618]

Arany Z, Lebrasseur N, Morris C, Smith E, Yang W, Ma Y, Chin S, Spiegelman BM. The transcriptional coactivator PGC-1beta drives the formation of oxidative type IIX fibers in skeletal muscle. Cell Metab. 2007; 5:35–46. [PubMed: 17189205]

Axell AM, MacLean HE, Plant DR, Harcourt LJ, Davis JA, Jimenez M, Handelsman DJ, Lynch GS, Zajac JD. Continuous testosterone administration prevents skeletal muscle atrophy and enhances resistance to fatigue in orchidectomized male mice. Am J Physiol Endocrinol Metab. 2006; 291:E506–E516. [PubMed: 16621900]

Bodine SC, Latres E, Baumhueter S, Lai VK, Nunez L, Clarke BA, Poueymirou WT, Panaro FJ, Na E, Dharmarajan K, et al. Identification of ubiquitin ligases required for skeletal muscle atrophy. Science. 2001; 294:1704–1708. [PubMed: 11679633]

Busquets S, Toledo M, Orpi M, Massa D, Porta M, Capdevila E, Padilla N, Frailis V, Lopez-Soriano FJ, Han HQ, et al. Myostatin blockage using actRIIB antagonism in mice bearing the Lewis lung carcinoma results in the improvement of muscle wasting and physical performance. J Cachexia Sarcopenia Muscle. 2012; 3:37–43. [PubMed: 22450815]

Chakkalakal JV, Nishimune H, Ruas JL, Spiegelman BM, Sanes JR. Retrograde influence of muscle fibers on their innervation revealed by a novel marker for slow motoneurons. Development. 2010; 137:3489–3499. [PubMed: 20843861]

Chinsomboon J, Ruas J, Gupta RK, Thom R, Shoag J, Rowe GC, Sawada N, Raghuram S, Arany Z. The transcriptional coactivator PGC-1alpha mediates exercise-induced angiogenesis in skeletal muscle. Proc Natl Acad Sci U S A. 2009; 106:21401–21406. [PubMed: 19966219]

Choi CS, Befroy DE, Codella R, Kim S, Reznick RM, Hwang YJ, Liu ZX, Lee HY, Distefano A, Samuel VT, et al. Paradoxical effects of increased expression of PGC-1alpha on muscle mitochondrial function and insulin-stimulated muscle glucose metabolism. Proc Natl Acad Sci U S A. 2008; 105:19926–19931. [PubMed: 19066218]

Das SK, Eder S, Schauer S, Diwoky C, Temmel H, Guertl B, Gorkiewicz G, Tamilarasan KP, Kumari P, Trauner M, et al. Adipose triglyceride lipase contributes to cancer-associated cachexia. Science. 2011; 333:233–238. [PubMed: 21680814]

Dinchuk JE, Cao C, Huang F, Reeves KA, Wang J, Myers F, Cantor GH, Zhou X, Attar RM, Gottardis M, et al. Insulin receptor (IR) pathway hyperactivity in IGF-IR null cells and suppression of downstream growth signaling using the dual IGF-IR/IR inhibitor, BMS-754807. Endocrinology. 2010; 151:4123–4132. [PubMed: 20610571]

Fearon KC, Glass DJ, Guttridge DC. Cancer Cachexia: Mediators, Signaling, and Metabolic Pathways. Cell Metab. 2012

Florini JR. Hormonal control of muscle growth. Muscle Nerve. 1987; 10:577–598. [PubMed: 3309650]

Gentry BA, Ferreira JA, Phillips CL, Brown M. Hindlimb skeletal muscle function in myostatin-deficient mice. Muscle Nerve. 2011; 43:49–57. [PubMed: 21082689]

Giguere V. Transcriptional control of energy homeostasis by the estrogen-related receptors. Endocr Rev. 2008; 29:677–696. [PubMed: 18664618]

Gomes MD, Lecker SH, Jagoe RT, Navon A, Goldberg AL. Atrogin- 1, a muscle-specific F-box protein highly expressed during muscle atrophy. Proc Natl Acad Sci U S A. 2001; 98:14440–14445. [PubMed: 11717410]

Handschin C, Choi CS, Chin S, Kim S, Kawamori D, Kurpad AJ, Neubauer N, Hu J, Mootha VK, Kim YB, et al. Abnormal glucose homeostasis in skeletal muscle-specific PGC-1alpha knockout mice reveals skeletal muscle-pancreatic beta cell crosstalk. J Clin Invest. 2007; 117:3463–3474. [PubMed: 17932564]

Hanson AM, Stodieck LS, Cannon CM, Simske SJ, Ferguson VL. Seven days of muscle re-loading and voluntary wheel running following hindlimb suspension in mice restores running performance, muscle morphology and metrics of fatigue but not muscle strength. J Muscle Res Cell Motil. 2010; 31:141–153. [PubMed: 20632203]

Heard E, Rougeulle C, Arnaud D, Avner P, Allis CD, Spector DL. Methylation of histone H3 at Lys-9 is an early mark on the X chromosome during X inactivation. Cell. 2001; 107:727–738. [PubMed: 11747809]

Iezzi S, Di Padova M, Serra C, Caretti G, Simone C, Maklan E, Minetti G, Zhao P, Hoffman EP, Puri PL, et al. Deacetylase inhibitors increase muscle cell size by promoting myoblast recruitment and fusion through induction of follistatin. Dev Cell. 2004; 6:673–684. [PubMed: 15130492]

Lee SJ. Regulation of muscle mass by myostatin. Annu Rev Cell Dev Biol. 2004; 20:61–86. [PubMed: 15473835]

Lee SJ. Quadrupling muscle mass in mice by targeting TGF-beta signaling pathways. PLoS One. 2007; 2:e789. [PubMed: 17726519]

McMillan DN, Noble BS, Maltin CA. The effect of the beta-adrenergic agonist clenbuterol on growth and protein metabolism in rat muscle cell cultures. J Anim Sci. 1992; 70:3014–3023. [PubMed: 1429278]

McPherron AC, Lawler AM, Lee SJ. Regulation of skeletal muscle mass in mice by a new TGF-beta superfamily member. Nature. 1997; 387:83–90. [PubMed: 9139826]

Megeney LA, Perry RL, LeCouter JE, Rudnicki MA. bFGF and LIF signaling activates STAT3 in proliferating myoblasts. Dev Genet. 1996; 19:139–145. [PubMed: 8900046]

Mendias CL, Marcin JE, Calerdon DR, Faulkner JA. Contractile properties of EDL and soleus muscles of myostatin-deficient mice. J Appl Physiol. 2006; 101:898–905. [PubMed: 16709649]

Mir LM, Bureau MF, Gehl J, Rangara R, Rouy D, Caillaud JM, Delaere P, Branellec D, Schwartz B, Scherman D. High-efficiency gene transfer into skeletal muscle mediated by electric pulses. Proc Natl Acad Sci U S A. 1999; 96:4262–4267. [PubMed: 10200250]

Nair KS. Aging muscle. Am J Clin Nutr. 2005; 81:953–963. [PubMed: 15883415]

Ogryzko VV, Schiltz RL, Russanova V, Howard BH, Nakatani Y. The transcriptional coactivators p300 and CBP are histone acetyltransferases. Cell. 1996; 87:953–959. [PubMed: 8945521]

Pende M, Um SH, Mieulet V, Sticker M, Goss VL, Mestan J, Mueller M, Fumagalli S, Kozma SC, Thomas G. S6K1(−/−)/S6K2(−/−) mice exhibit perinatal lethality and rapamycin-sensitive 5'-terminal oligopyrimidine mRNA translation and reveal a mitogen-activated protein kinase-dependent S6 kinase pathway. Mol Cell Biol. 2004; 24:3112–3124. [PubMed: 15060135]

Sandri M, Lin J, Handschin C, Yang W, Arany ZP, Lecker SH, Goldberg AL, Spiegelman BM. PGC-1alpha protects skeletal muscle from atrophy by suppressing FoxO3 action and atrophy-specific gene transcription. Proc Natl Acad Sci U S A. 2006; 103:16260–16265. [PubMed: 17053067]

Schiaffino S, Mammucari C. Regulation of skeletal muscle growth by the IGF1-Akt/PKB pathway: insights from genetic models. Skelet Muscle. 2011; 1:4. [PubMed: 21798082]

Short KR, Vittone JL, Bigelow ML, Proctor DN, Rizza RA, Coenen-Schimke JM, Nair KS. Impact of aerobic exercise training on age-related changes in insulin sensitivity and muscle oxidative capacity. Diabetes. 2003; 52:1888–1896. [PubMed: 12882902]

Tadaishi M, Miura S, Kai Y, Kano Y, Oishi Y, Ezaki O. Skeletal muscle-specific expression of PGC-1alpha-b, an exercise-responsive isoform, increases exercise capacity and peak oxygen uptake. PLoS One. 2011; 6:e28290. [PubMed: 22174785]

Wende AR, Schaeffer PJ, Parker GJ, Zechner C, Han DH, Chen MM, Hancock CR, Lehman JJ, Huss JM, McClain DA, et al. A role for the transcriptional coactivator PGC-1alpha in muscle refueling. J Biol Chem. 2007; 282:36642–36651. [PubMed: 17932032]

Wenz T, Rossi SG, Rotundo RL, Spiegelman BM, Moraes CT. Increased muscle PGC-1alpha expression protects from sarcopenia and metabolic disease during aging. Proc Natl Acad Sci U S A. 2009; 106:20405–20410. [PubMed: 19918075]

White JP, Baynes JW, Welle SL, Kostek MC, Matesic LE, Sato S, Carson JA. The regulation of skeletal muscle protein turnover during the progression of cancer cachexia in the Apc(Min/+) mouse. PLoS One. 2011; 6:e24650. [PubMed: 21949739]

Yoshioka T, Inagaki K, Noguchi T, Sakai M, Ogawa W, Hosooka T, Iguchi H, Watanabe E, Matsuki Y, Hiramatsu R, et al. Identification and characterization of an alternative promoter of the human PGC-1alpha gene. Biochem Biophys Res Commun. 2009; 381:537–543. [PubMed: 19233136]

Zhang Y, Huypens P, Adamson AW, Chang JS, Henagan TM, Boudreau A, Lenard NR, Burk D, Klein J, Perwitz N, et al. Alternative mRNA splicing produces a novel biologically active short isoform of PGC-1alpha. J Biol Chem. 2009; 284:32813–32826. [PubMed: 19773550]

Research Highlights

1. Three PGC-1α variants generated by alternative promoter use and alternative splicing
2. PGC-1α4 induces skeletal muscle hypertrophy
3. PGC-1α4 muscle-specific transgenics have increased muscle mass and strength
4. PGC-1α4 transgenic mice are resistant to cancer-induced cachexia

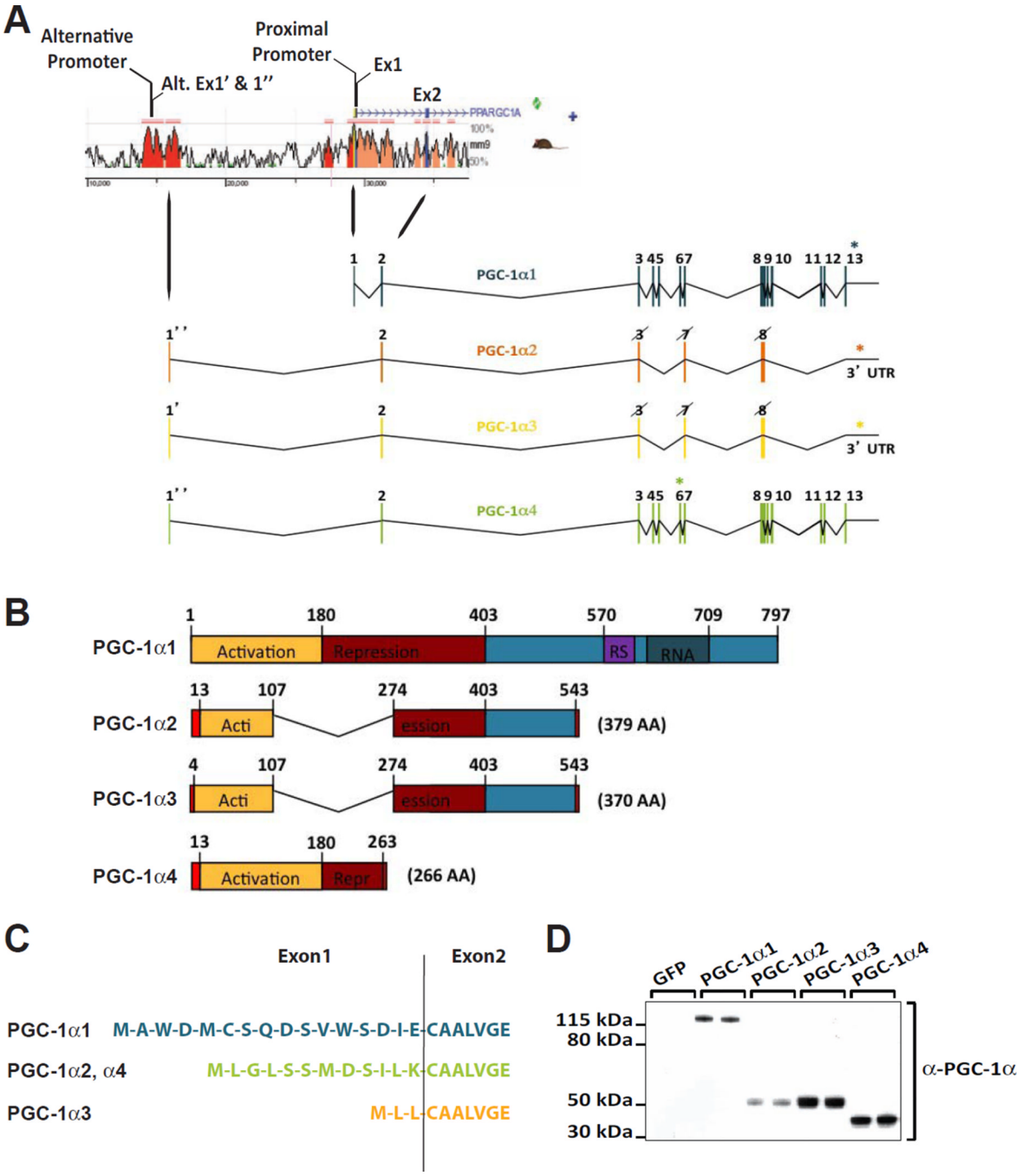

Figure 1. Cloning and characterization of novel PGC-1α isoforms

(A) Schematic representation of the conservation between human and mouse PGC-1α gene (www.dcode.org). Two promoters that can drive expression of the PGC-1α gene. (Ex) indicates exons seen in the depicted region. Structure of the different PGC-1α isoform mRNA is shown. / indicates partial conservation. * stop codon.

(B) PGC-1α protein domain conservation. Amino acid numbers refer to mouse PGC-1α (hereafter PGC-1α1). Numbers in brackets indicate the number of amino acids for each isoform. Red boxes indicate new N- and C-terminal amino acid sequences.

(C) Three different exon1 coding sequences result in different N-terminal amino acid sequences. PGC-1α2 and α4 share the same alternative exon1, and therefore the same first 12 amino acids. All isoforms share exon2.
(D) Differential promoter usage and splicing options result in proteins with different molecular weights. The different PGC-1α isoforms were expressed in HEK293 cells. Whole-cell extracts were resolved by SDS PAGE followed by immunoblotting using an anti-PGC-1α antibody (Zhang et al., 2009) that we have found to recognize all isoforms described here. See also Figure S1.

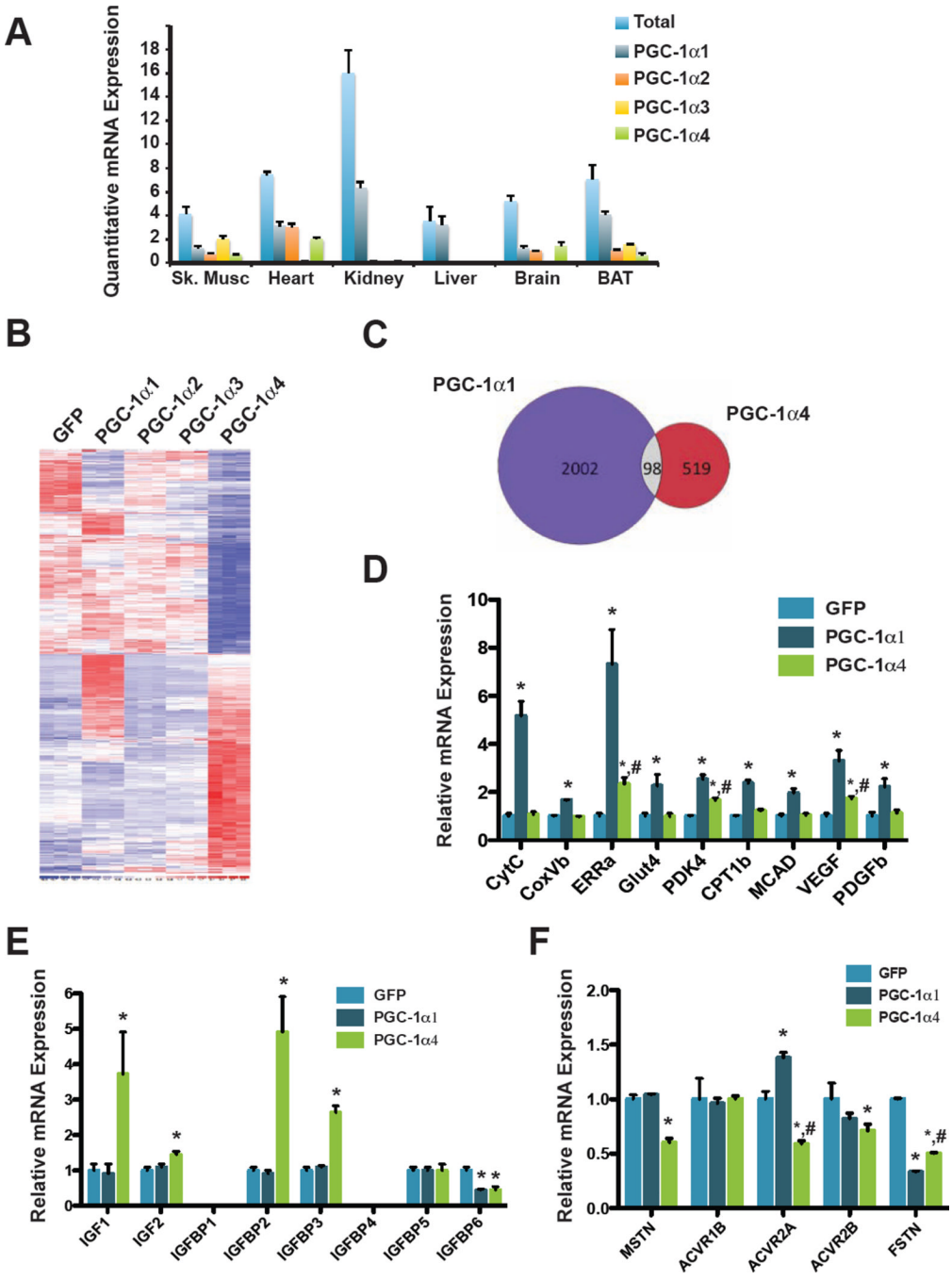

Figure 2. Gene expression profiling of PGC-1α isoforms and their target genes

(A) Tissue-specific PGC-1α isoform expression patterns. Absolute quantification of gene expression in mouse tissues (n=6) by qRT-PCR using isoform-specific primers.

(B) Heat map summary of relative changes in gene expression by each PGC-1α isoform. Gene expression was analyzed (affymetrix) in myotubes expressing GFP alone (control), or together with each PGC-1α isoform. Experiments were performed in triplicate and results were analyzed with dChip software.

(C) Venn diagram represents the number of genes regulated by PGC-1α1, PGC-1α4, and in common between both isoforms.

(D, E, and F) From the Affymetrix results, gene sets were validated by qRT-PCR using specific primers. RNA was prepared as described in (B). Bars depict mean values and error bars represent standard deviation. *, $p < 0.05$ between indicated group and control. *,#, $p < 0.05$ between all groups. See also Figure S2.

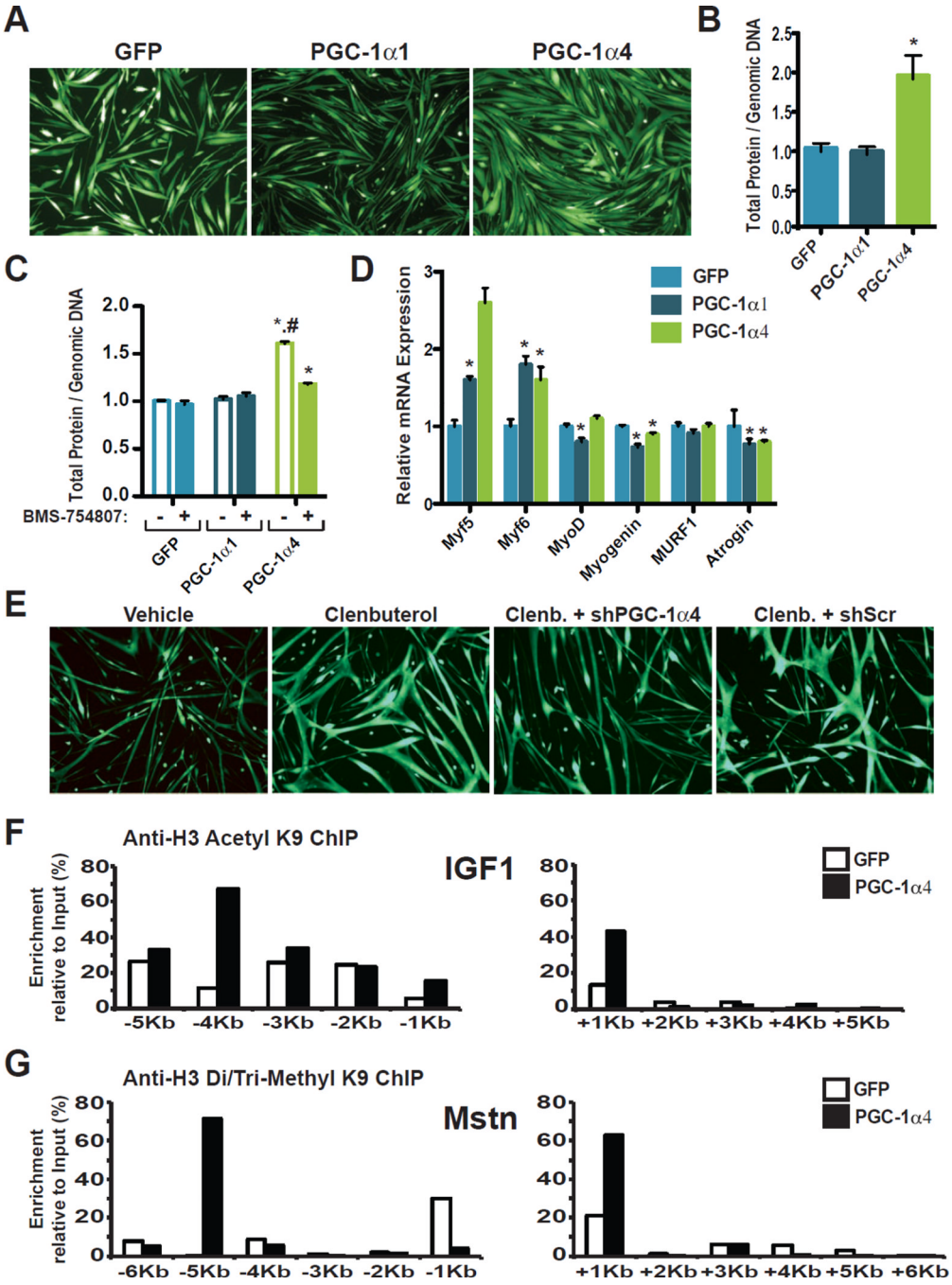

Figure 3. Myotubes expressing PGC-1α4 show cellular hypertrophy

(A) Fluorescence microscopy analysis of myotubes expressing GFP alone, or together with PGC-1α1 or PGC-1α4. Fully differentiated myotubes were transduced with the different adenovirus and observed under a fluorescence microscope 36 hours later with a 10X objective.

(B) Protein accumulation normalized by genomic DNA content in myotubes expressing GFP control, PGC-1α1 or PGC-1α4. Experiments were performed as described in (A) but cells were processed for either total protein or DNA quantification. Graphs show the total protein/genomic DNA ratio.

(C) Protein accumulation normalized by genomic DNA content in myotubes expressing GFP control, PGC-1α1 or PGC-1α4 and treated with the IGF1R inhibitor BMS-754807. Myotubes were transduced as described in (A) and treated with 5 nM BMS-754807. At the end of 36 hours cells were processed for total protein or DNA quantification.
(D) Analysis of gene expression for markers of myogenic differentiation. Experiments were performed as described in (A) and gene expression analyzed by qRT-PCR using primers specific to the indicated genes.
(E) PGC-1α4 loss-of-function blunts clenbuterol-induced myotube hypertrophy. Fully differentiated primary myotubes were treated with 500 nM Clenbuterol (or vehicle) and transduced with adenovirus expressing PGC-1α4-specific or scrambled control shRNAs. 48 hours later, cells were processed for fluorescence microscopy or analysis of protein/DNA content.
(F) Chromatin immunoprecipitation (ChIP) of DNA regions associated with Acetyl-H3K9. Myotubes expressing GFP alone or with PGC-1α4 were processed for chromatin immunoprecipitation. Purified DNA fragments were identified and quantified by PCR using primers targeting the IGF1 gene at 1 kb intervals. Graph shows enrichment relative to input after normalized by IgG.
(G) ChIP of regions associated with di/trimethyl-H3K9. Myotubes were processed as described above. Purified DNA fragments were identified and quantified by PCR using primers targeting the Myostatin gene at 1 kb intervals. Graph shows enrichment relative to input normalized by IgG.
Bars depict mean values and error bars represent standard deviation. *, $p < 0.05$ between indicated group and control. $^{*,\#}$, $p < 0.05$ between all groups. See also Figure S3.

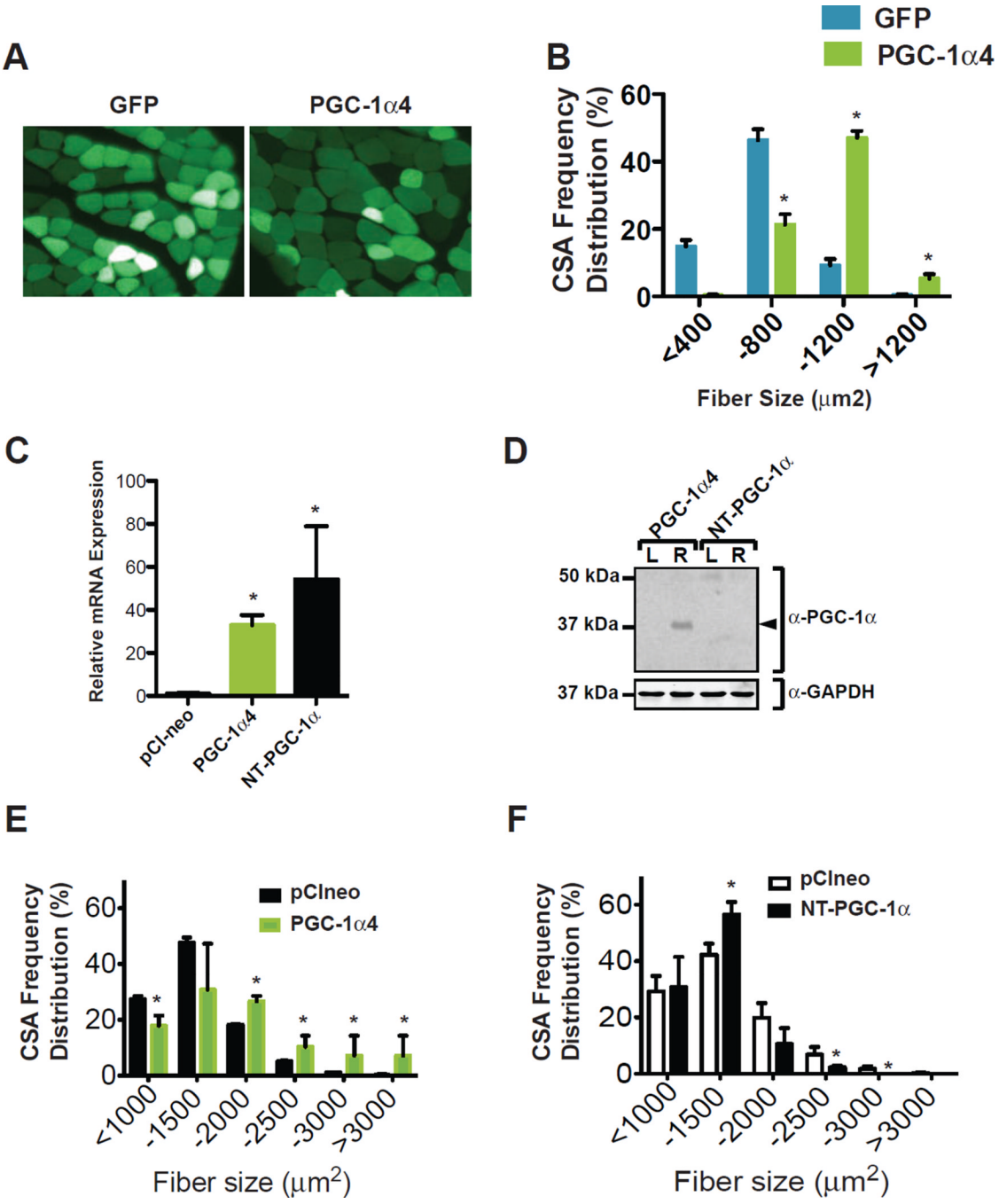

Figure 4. In vivo expression of PGC-1α4 induces skeletal muscle hypertrophy

(A) Adenovirus-mediated expression of PGC-1α4 in mouse skeletal muscle. Cross-section of the gastrocnemius muscle, seven days after intramuscular injection of adenovirus expressing GFP alone or with PGC-1α4.

(B) Cross-sectional area frequency distribution (sections from 6 mice per group).

(C) PGC-1α4 and NT-PGC-1α mRNA expression levels in electroporated tibialis anterior analyzed by qRT-PCR using primers targeting exon 2 (present in both isoforms).

(D) PGC-1α4 and NT-PGC-1α protein expression levels in electroporated muscle.

(E, F) Electroporation-mediated delivery of plasmids into the tibialis anterior (TA). Each mouse (n=6 per group) received a control plasmid in one limb (pCI-neo), and in the

contralateral limb the plasmid encoding PGC-1α4 or NT-PGC-1α. Bars depict mean values and error bars represent standard error. *, $p < 0.05$ between indicated group and control. See also Figure S4.

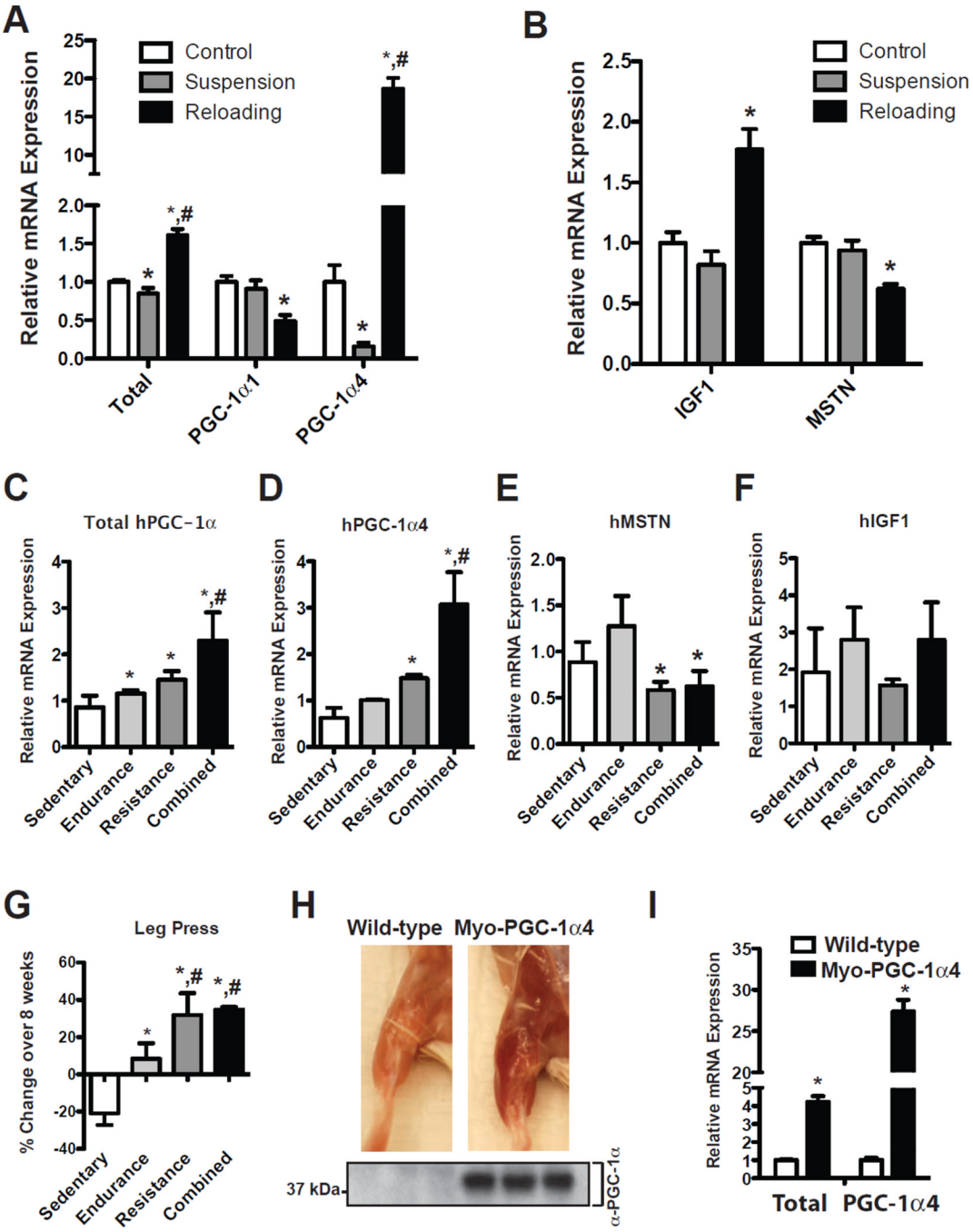

Figure 5. PGC-1α4 expression increases during muscle hypertrophy and resistance training

(A,B) PGC-1α4 expression increases during the hypertrophy phase of a suspension/reloading protocol. C57Bl/6 mice were divided into groups (n=4 each): control, 10 days hindlimb suspension (Suspension), or 10 days suspension plus 24 hours of reloading (Reloading). The soleus muscles were harvested and processed for gene expression analysis by qRT-PCR using primers specific for the indicated genes.

(C–F) Analysis of gene expression in skeletal muscle biopsies from human volunteers. Percutaneous vastuls lateralis biopsies were obtained at baseline and eight weeks later, ~48h after the last training session. Gene expression was analyzed by qRT-PCR using primers specific to the indicated genes.

(G) Increase in PGC-1α4 expression correlates with improvement in leg press exercise performance. Graph shows the percent change in the number of leg press repetitions observed between baseline and after 8 weeks of training.
(H) Morphology of hindlimbs from wild-type and PGC-1α4 transgenic mice (Myo-PGC-1α4). Immunoblot using an anti-PGC-1α antibody (α-PGC-1α) shows PGC-1α4 protein levels in the gastrocnemius muscle.
(I) Total PGC-1α and PGC-1α4 mRNA levels in the Myo-PGC-1α4 mouse line were determined by qRT-PCR and compared to the wild-type littermate controls. Bars depict mean values and error bars represent standard deviation. *, $p < 0.05$ between indicated group and control. $^{*,\#}$, $p < 0.05$ between all groups.

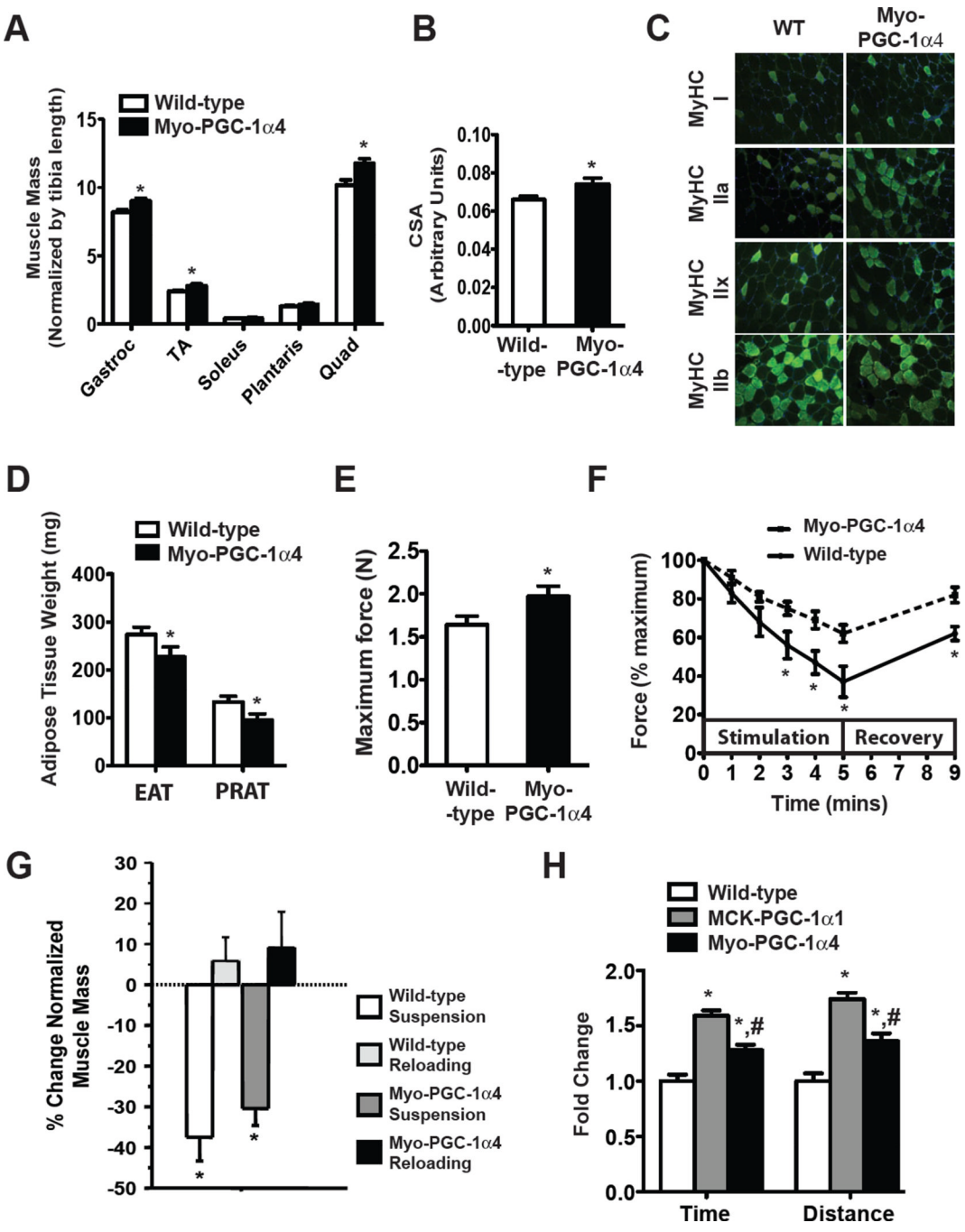

Figure 6. Myo-PGC-1α4 skeletal muscle transgenics have increased muscle mass and strength

(A) Determination of muscle wet weight from PGC-1α4 transgenics and wild-type controls (n=6). Muscle weights are normalized by tibia length.

(B) Fiber cross-sectional area in the gastrocnemius muscle of wild-type and PGC-1α4 transgenics.

(C) Immunohistochemical analysis of gastrocnemius muscle from wild-type (WT) and Myo-PGC-1α4 animals using antibodies against different myosin heavy chain (MyHC) types.

(D) Determination of Epididimal (EAT) and Peri-renal (PRAT) adipose tissue wet weight from PGC-1α4 transgenics and wild-type controls (n=6).

(E) Maximal force measurements of the gastrocnemius muscle of wild-type and PGC1α4 transgenics (Myo-PGC-1α4).
(F) Muscle fatigue test performed under the same experimental settings as in (E).
(G) Changes in normalized muscle mass with hindlimb suspension/reloading. N= 4 per group.
(H) Exercise tolerance test. Muscle-specific PGC-1α1 (MCK-PGC-1α) and PGC-1α4 (Myo-PGC-1α4) transgenics ran to exhaustion on a treadmill. Data is normalized by values obtained with wild-type animals (n=6 per group). Bars depict mean values and error bars represent standard error. *, $p < 0.05$ between indicated group and control. $^{*,\#}$, $p < 0.05$ between all groups. See also Figure S6 and Table S1.

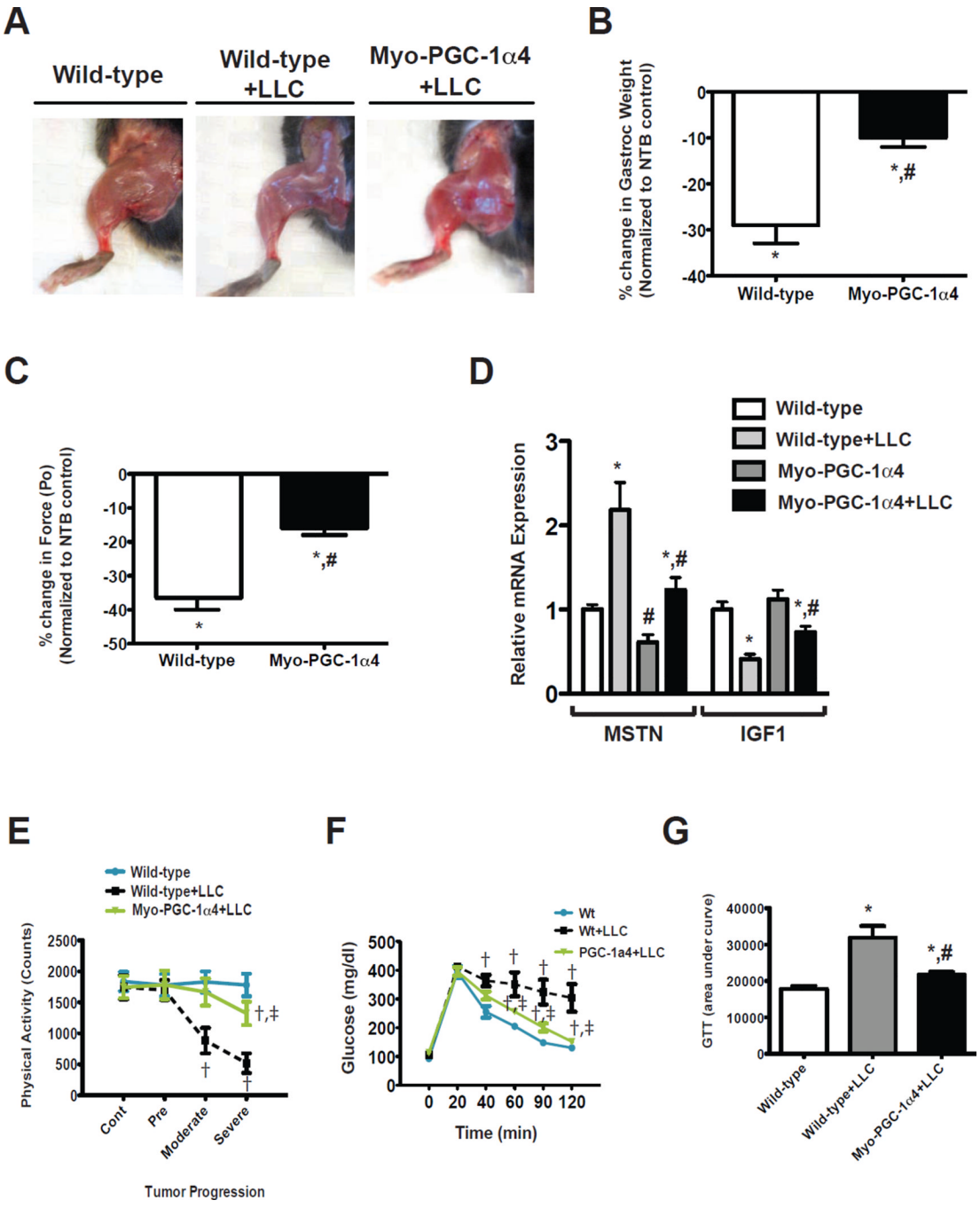

Figure 7. PGC-1α4 transgenic mice show resistance to muscle wasting during experimental cancer cachexia

(A) Representative images of hindlimb muscle muscles from wild-type, and tumor bearing (+LLC) wild-type or Myo-PGC-1α4 mice.

(B) Gastrocnemius muscle mass in wild-type and Myo-PGC-1α4 tumor bearing mice normalized to their own genotype non-tumor bearing control.

(C) Muscle force production in wild-type and Myo-PGC-1α4 tumor bearing mice normalized to their own genotype non tumor bearing control.

(D) Myostatin and IGF-1 mRNA expression in wild-type and Myo-PGC-1α4 with or without LLC tumor.

(E) Physical activity throughout the progression of tumor load.
(F) Glucose tolerance test.
(G) Quantification of glucose clearance. Bars depict mean values and error bars represent standard error. *, $p < 0.05$ between indicated group and its genotype control. #, $p < 0.05$ between indicated group and group receiving same treatment across genotypes. †, $p < 0.05$ between indicated group and wild-type mice. ‡, $p < 0.05$ between indicated group and wild-type + LLC mice. See also Figure S7.